Showcasing research from Professor Ranjit Thakuria's laboratory, Department of Chemistry, Gauhati University, Assam, India.

Beyond serendipity: uncovering novel ratiometric urea·24DHBA cocrystals through mechanochemistry and MicroED

Demonstrating how the combination of mechanochemistry and MicroED serves as an efficient tool for synthesizing elusive ratiometric urea·24DHBA cocrystals

Image reproduced by permission of Ranjit Thakuria from *Chem. Commun.*, 2025, **61**, 16198.

As featured in:
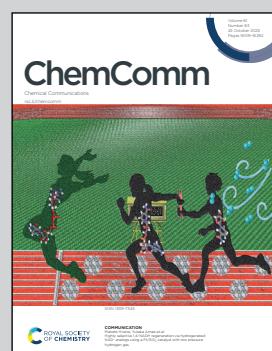
See Toshiyuki Sasaki,
Genji Kurisu, Ranjit Thakuria *et al.*,
Chem. Commun., 2025, **61**, 16198.

ROYAL SOCIETY
OF **CHEMISTRY**

rsc.li/chemcomm

Check for updates

Beyond serendipity: uncovering novel ratiometric urea·24DHBA cocrystals through mechanochemistry and MicroED

Ankur Bonia,[a] Diptajyoti Gogoi,[a] Nabadeep Kalita,[a] Takanori Nakane, [bc] Akihiro Kawamoto, [bc] Khaled Althubeiti, [d] Toshiyuki Sasaki, [*e] Genji Kurisu [*bcf] and Ranjit Thakuria [*ag]

Mechanochemical synthesis of urea cocrystals with 2,4-dihydroxy-benzoic acid (24DHBA) reveals two new stoichiometric forms: (urea)$_2$·(24DHBA) and (urea)$_2$·(24DHBA)$_2$, not accessible *via* solution methods. The known (urea)$_{0.5}$·(24DHBA) form remains the most stable. These findings provide critical insights into stoichiometric tuning of agro-cocrystals and pave the way for their practical application in sustainable agriculture.

Impurities pose a significant challenge not only during the synthesis but also throughout large-scale manufacturing.[1,2] Their presence, whether as unwanted polymorphs, by-products, or unreacted starting materials, can adversely affect the physico-chemical properties of the final product. This, in turn, may lead to batch rejection or, in severe cases, market withdrawal.[3] The importance of impurity identification is thus paramount during process development and scale-up manufacturing.[4] Well-known cases, such as the metastable polymorph of ritonavir,[3] or rifaximin,[5,6] highlight the critical impact that even trace impurities can have on drug performance and regulatory acceptance. To mitigate such risks, it is a standard practice to explore both the crystal structure landscape and the energy landscape of disappearing polymorphs,[7–11] alongside the investigation of various solid-state formulations[12] such as cocrystals, solvates, hydrates, and reaction intermediates.[13] These strategies are routinely employed during

scale-up manufacturing.[3,14–19] While such approaches are well-established for single-component systems, the complexity increases considerably when dealing with multicomponent systems like cocrystals. This complexity arises from the wide range of possible solid forms generated during co-crystallization, including cocrystal hydrates, cocrystal solvates, salt–cocrystal hybrids, salt solvates,[20] ratiometric cocrystals,[21,22] and polymorphs of all possible multi-component solids,[23] among others.[24–28]

The spontaneity of cocrystal nucleation is closely tied to the activation energy (E_a) of the system. Typically, solution crystallization favors the formation of thermodynamically stable cocrystals. In contrast, alternative techniques such as melt crystallization, sublimation, supercritical CO$_2$ anti-solvent methods, freeze-drying, and mechanochemistry can often yield kinetically stable forms.[29,30] This distinction has been well-articulated in a recent highlight by Wong *et al.*[4] Recent investigations have increasingly focused on agro-based cocrystals due to their potential application as alternative fertilizers with sustained-release properties.[31–33] As a result, the development of scalable synthesis methods for these materials is essential for enabling field trials. Among the various approaches, mechanochemical synthesis has emerged as one of the most efficient and environmentally benign techniques for large-scale preparation.[8,11,19,26,28,30]

In continuation to one of our recent studies[34] on mechanochemical synthesis and sustained release behavior of urea–hydroxybenzoic acid cocrystals, we report here the discovery of two previously elusive urea·24DHBA cocrystals. Through high-throughput mechanochemical screening combined with micro-crystal electron diffraction (MicroED), an efficient tool for small molecule characterization,[35] we were able to resolve their crystal structures and determine their precise stoichiometries. Furthermore, we systematically explored the influence of various mechanochemical parameters such as milling time, milling frequency, nature and volume of liquid additives (η), and reactant stoichiometry on the product formation. These studies provide critical insights into the mechanistic aspects of cocrystal formation and open up new avenues for the rational design of agro-based cocrystal materials.

[a] *Department of Chemistry, Gauhati University, Guwahati 781014, India.*
 E-mail: ranjit.thakuria@gauhati.ac.in, ranjit.thakuria@gmail.com

[b] *Institute for Protein Research, Osaka University, 3-2 Yamadaoka, Suita, Osaka 565-0871, Japan. E-mail: gkurisu@protein.osaka-u.ac.jp*

[c] *JEOL YOKOGUSHI Research Alliance Laboratories, Graduate School of Frontier Biosciences, Osaka University, 1-3 Yamadaoka, Suita, Osaka 565-0871, Japan. E-mail: gkurisu@protein.osaka-u.ac.jp*

[d] *Department of Chemistry, College of Science, Taif University, Taif 21944, Saudi Arabia*

[e] *Japan Synchrotron Radiation Research Institute (JASRI), 1-1-1 Kouto, Sayo-cho, Sayo-gun, Hyogo 679-5198, Japan. E-mail: toshiyuki.sasaki@spring8.or.jp*

[f] *Institute for Open and Transdisciplinary Research Initiatives, Osaka University, 2-1 Yamadaoka, Suita, Osaka 565-0871, Japan*

[g] *Faculty of Chemistry, University of Warsaw, 1 Pasteura Street, 02-093 Warsaw, Poland*
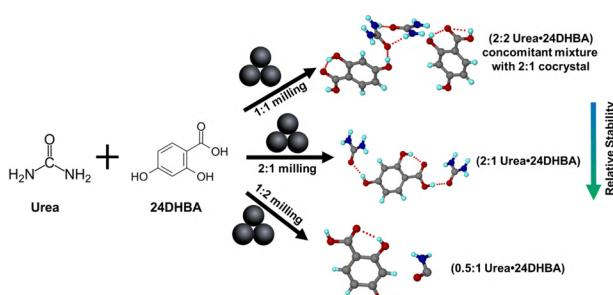
Scheme 1 Formation of ratiometric cocrystals under different milling environments, summarizing the present study and our previous report.[34]

In our previous report, we characterized a urea cocrystal with 24DHBA, synthesized *via* mechanochemistry. The resulting cocrystal, with a stoichiometry of (urea)$_{0.5}$·(24DHBA), demonstrates high stability under 75% relative humidity as well as during solubility analysis. Notably, it does not undergo any phase transformation or cocrystal dissociation under various environmental conditions. Since solution crystallization from even a 1 : 1 stoichiometric mixture consistently yields a 0.5 : 1 cocrystal, we reinvestigated the potential for stoichiometric modulation using liquid-assisted grinding (LAG) (Scheme 1). Powder X-ray diffraction (PXRD) of ground samples prepared in a Retsch Mixer Mill (MM400) by mixing 1 : 1 stoichiometry of urea (20.2 mg, 0.33 mmol) and 24DHBA (51.37 mg, 0.33 mmol) in a 5 mL stainless-steel milling jar along with two 7 mm stainless-steel grinding balls in the presence of 150 μL (η = 2.1) of various added liquids for 30 min at a frequency of 20 Hz showed the appearance of a few new diffraction peaks (Fig. S1). After several batches of failed crystallization, MicroED was used as a characterization tool to determine the crystal structure of the elusive 1 : 1 cocrystal.

In the reported (urea)$_{0.5}$·(24DHBA) cocrystal, the asymmetric unit comprises half a molecule of urea and one molecule of

24DHBA (Fig. 1(a)). The crystal structure was solved in the orthorhombic *Pnma* space group, with no direct interactions observed between urea molecules. Instead, the two amino groups and the carbonyl group of urea engage in hydrogen bonding with the *para*-hydroxyl group of 24DHBA, forming an infinite molecular tape parallel to the *a*-axis. The carboxylic acid groups of 24DHBA form centrosymmetric acid–acid homo-dimers, which link antiparallel urea–24DHBA tapes from different molecular planes, resulting in a three-dimensional (3D) network structure (Fig. 1(b)).

In contrast, MicroED structural analysis of the 1 : 1 stoichiometric powder mixture revealed the presence of two molecules each of urea and 24DHBA in the asymmetric unit (Fig. 1(c)). This new cocrystal, henceforth referred to as (urea)$_2$·(24DHBA)$_2$, crystallizes in the $P2_1/n$ space group with unit cell parameters a = 6.9711 Å, b = 11.059 Å, c = 31.307 Å, α = 90°, β = 91.70°, γ = 90°, and V = 2412.6 Å³. Unlike the previously reported structure, this form features an infinite urea tape along the *a*-axis, in which urea molecules are connected *via* an amide–amide dimer synthon (Fig. 1(e)). The two symmetry-independent 24DHBA molecules link the urea tape through O–H···O and O···H–N hydrogen bonds *via* their hydroxyl groups. Parallel urea tapes are further bridged by these 24DHBA molecules through acid–acid homodimers, forming a layered structure. In 3D, the 24DHBA dimer units connect adjacent urea tapes, resulting in a 3D molecular grid architecture (Fig. 1(f)).

Interestingly, during MicroED structure elucidation of mechanically ground powder samples of the 1 : 1 urea–24DHBA mixture, some crystals had different unit cell parameters. These correspond to a 2 : 1 cocrystal, hereafter referred to as (urea)$_2$·(24DHBA). The crystal structure, solved in the $P\bar{1}$ space group, contains two molecules of urea and one molecule of 24DHBA in the asymmetric unit (Fig. 1(g) and (h)). The unit cell parameters are a = 7.2558 Å, b = 8.8651 Å, c = 10.860 Å, α = 74.412°, β = 75.956°, γ = 71.464°, with a unit cell volume of V = 628.4 Å³. Similar to the (urea)$_2$·(24DHBA)$_2$ cocrystal, this (urea)$_2$·(24DHBA) structure
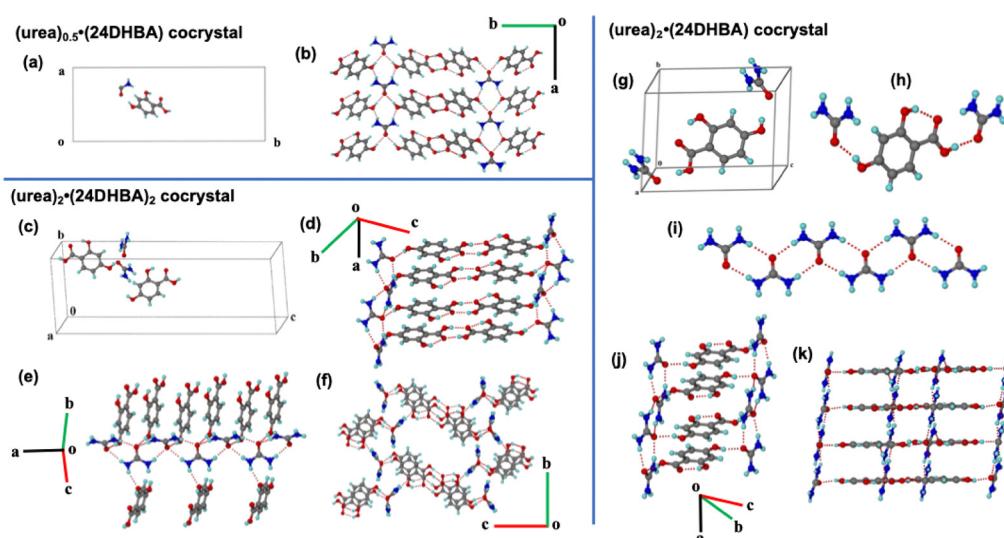

Fig. 1 Crystal packing and hydrogen bond interactions present in the variable stoichiometric cocrystals of urea with 24DHBA, respectively (a) and (b) (urea)$_{0.5}$·(24DHBA); (c)–(f) (urea)$_2$·(24DHBA)$_2$ and (g)–(k) (urea)$_2$·(24DHBA).

features infinite tapes of urea molecules aligned parallel to the *a*-axis, formed *via* amide–amide dimer synthons (Fig. 1(i)). However, unlike the other forms, this cocrystal does not exhibit the characteristic acid–acid dimer synthon. Instead, the carboxylic acid and *para*-hydroxyl groups of the 24DHBA coformer bridge two symmetry-independent urea molecules from opposite directions, forming a two-dimensional ladder-like motif (Fig. 1(j)). Additionally, an intra-molecular hydrogen bond between the 2-hydroxyl group and the carbonyl oxygen of 24DHBA facilitates further linkage of neighboring urea tapes, resulting in a 2D square grid network (Fig. 1(k)). Crystal-lographic and hydrogen bond parameters of all the urea·24DHBA cocrystals are summarized in Tables S1 and S2, respectively.

We investigated the formation of different stoichiometries by varying the amount of the organic liquid, THF, during LAG. Milling equimolar (1:1) amounts of urea and 24DHBA in the presence of varying amounts of THF yielded different product mixtures. Specifically, using THF volumes corresponding to η values between 0.54 and 2.1 resulted in a mixture of reported $(urea)_{0.5}\cdot(24DHBA)$ and $(urea)_2\cdot(24DHBA)$ cocrystals (Fig. S2a). In contrast, η values between 2.8 and 8.4 led to a mixture of $(urea)_2\cdot(24DHBA)_2$ and $(urea)_2\cdot(24DHBA)$ cocrystals (Fig. S2b). Interestingly, milling with a 2:1 stoichiometric ratio of urea to 24DHBA under various THF volumes consistently yielded a pure phase of the resulting material, *i.e.* a $(urea)_2\cdot(24DHBA)$ cocrystal (Fig. S2c).

The hydration stability of the synthesized urea cocrystals was evaluated by storing the powder samples in a bell jar at 75% RH (achieved using a saturated aqueous sodium chloride (NaCl) solution) and ambient temperature. PXRD analysis was conducted periodically over a duration of 45 days. No significant changes were observed in the PXRD patterns of the phase pure $(urea)_{0.5}\cdot(24DHBA)$ and $(urea)_2\cdot(24DHBA)$ cocrystals upon prolonged storage, even after 45 days. Due to the challenges in obtaining a bulk pure sample of the $(urea)_2\cdot(24DHBA)_2$ cocrystal, a powder mixture containing both $(urea)_2\cdot(24DHBA)_2$ and $(urea)_2\cdot(24DHBA)$ cocrystals was used. PXRD analysis revealed the emergence of peaks corresponding to the reported $(urea)_{0.5}\cdot(24DHBA)$ cocrystal after 30 days, indicating a phase transformation and metastable nature of the $(urea)_2\cdot(24DHBA)_2$ cocrystal (Fig. S3).

Hirshfeld surface analysis is a powerful tool to explore intermolecular interactions within a crystal structure, and visualize and quantify how molecules pack together and interact in the solid-state.[36–39] The parameters d_i and d_e signify the distance from the Hirshfeld surface to the nearest internal and external atoms, respectively. And the normalized contact distance d_{norm} is defined as

$$d_{norm} = d_{|e|} + d_{|i|}$$

where, $d_{|e|} = (d_e - r_{vdw})/r_{vdw}$ and $d_{|i|} = (d_i - r_{vdw})/r_{vdw}$ and r_{vdw} corresponds to the van der Waals radius of the atom involved.

To investigate the relative stability of the ratiometric cocrystals, we performed Hirshfeld surface analysis on all the urea·24DHBA cocrystals and generated their corresponding 2D fingerprint plots (Fig. S4). By quantifying the contributions of various intermolecular interactions (Fig. 2), we observed that the O···H hydrogen bonding interactions (blue bar) exhibited the highest contribution of strong non-covalent interactions to
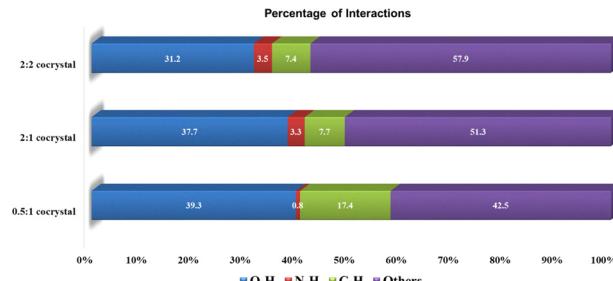

Fig. 2 Percentage contributions of various intermolecular interactions present in the $(urea)_{0.5}\cdot(24DHBA)$, $(urea)_2\cdot(24DHBA)$ and $(urea)_2\cdot(24DHBA)_2$ cocrystals calculated based on Hirshfeld surface analysis fingerprint plots.

the Hirshfeld surface for all cocrystals analyzed. Specifically, the $(urea)_{0.5}\cdot(24DHBA)$ cocrystal showed the greatest contribution from O···H interactions at 39.3%, followed by $(urea)_2\cdot(24DHBA)$ at 37.7%, and the lowest in the $(urea)_2\cdot(24DHBA)_2$ cocrystal at 31.2%. These results highlight a trend in which the strength and prevalence of O···H interactions correlate with the relative thermodynamic stability of the cocrystals, i.e thermodynamic stability of the reported $(urea)_{0.5}\cdot(24DHBA)$ cocrystal and metastable nature of the $(urea)_2\cdot(24DHBA)_2$ cocrystal. Differential scanning calorimetry (DSC) analysis revealed a consistent trend, with the highest melting peak observed for the $(urea)_{0.5}\cdot(24DHBA)$ cocrystal, which also contained trace amounts of the other two stoichiometric cocrystals as impurities. In contrast, the lowest melting point corresponded to the metastable $(urea)_2\cdot(24DHBA)_2$ cocrystal (Fig. S5).

In summary, mechanochemical milling has enabled the discovery of two previously unreported ratiometric cocrystals alongside the well-established $(urea)_{0.5}\cdot(24DHBA)$ form. While conventional solution-based crystallization consistently yields this thermodynamically stable 0.5:1 cocrystal, the integration of mechanochemistry with MicroED revealed (Fig. S6 and S7) two elusive forms and allowed their structural characterization. Hirshfeld surface analysis and stability assessments confirmed that $(urea)_{0.5}\cdot(24DHBA)$ is the most stable form, with $(urea)_2\cdot(24DHBA)_2$ identified as metastable. The markedly higher aqueous solubility of urea relative to 24DHBA likely drives the selective formation of the 0.5:1 cocrystal during solution crystallization, even when starting from 1:1 or 2:1 stoichiometric mixtures. Interestingly, the metastable $(urea)_2\cdot(24DHBA)_2$ cocrystal was only observed during mechanochemical milling, consistently appearing as a minor, concomitant phase alongside the 1:2 and 2:1 cocrystals. However, extensive mechanochemical milling ultimately revealed the optimal conditions for the selective synthesis of the phase-pure $(urea)_2\cdot(24DHBA)$ cocrystal. These findings highlight a critical consideration for the large-scale production of cocrystals and other multicomponent solids: the necessity of identifying and controlling potential phase impurities. Our work underscores the value of comprehensive high-throughput screening across various stoichiometries and polymorphs, supplemented by detailed mapping of the energy landscape. Such an approach is essential to ensure batch consistency and to mitigate risks associated with unexpected phase impurities, including ratiometric cocrystals and undesired polymorphic forms.

In this context, the combined mechanochemistry and MicroED proves to be a highly sensitive and effective characterization strategy, capable of detecting even nanomolar-scale molecular impurities. This approach is especially valuable for quality assurance in the industrial-scale production of pharmaceutical and agrochemical multicomponent solids.

Conflicts of interest

There are no conflicts to declare.

Data availability

The detailed protocols and scripts for MicroED are in our GitHub repository (https://github.com/GKLabIPR/MicroED). Raw diffraction images are available at XRDa (ID: 390).

Supplementary information: Methods, PXRD data, crystallographic parameters, 2D fingerprint plots, and MicroED data. See DOI: https://doi.org/10.1039/d5cc03628c.

CCDC 2465561 (24DHBA), 2465562 ((urea)$_2$·(24DHBA)) and 2465472 ((urea)$_2$·(24DHBA)$_2$) contain the supplementary crystallographic data for this paper.[40a–c] Coordinates are also available from Crystallographic Open Database (accession: 3000604, 3000605, 3000606).

Notes and references

1 W. Kras, A. Carletta, R. Montis, R. A. Sullivan and A. J. Cruz-Cabeza, *Commun. Chem.*, 2021, **4**, 38.
2 D. Zheltikova, E. Losev and E. Boldyreva, *CrystEngComm*, 2023, **25**, 4879–4888.
3 S. R. Chemburkar, J. Bauer, K. Deming, H. Spiwek, K. Patel, J. Morris, R. Henry, S. Spanton, W. Dziki, W. Porter, J. Quick, P. Bauer, J. Donaubauer, B. A. Narayanan, M. Soldani, D. Riley and K. McFarland, *Org. Process Res. Dev.*, 2000, **4**, 413–417.
4 S. N. Wong, M. Fu, S. Li, W. T. C. Kwok, S. Chow, K.-H. Low and S. F. Chow, *CrystEngComm*, 2024, **26**, 1505–1526.
5 G. C. Viscomi, M. Campana, M. Barbanti, F. Grepioni, M. Polito, D. Confortini, G. Rosini, P. Righi, V. Cannata and D. Braga, *CrystEngComm*, 2008, **10**, 1074–1081.
6 A. Xu, Y. Xue, Y. Zeng, J. Li, H. Zhou, Z. Wang, Y. Chen, H. Chen, J. Jin and T. Zhuang, *Molecules*, 2023, **28**(5), 2415.
7 D.-K. Bučar, R. W. Lancaster and J. Bernstein, *Angew. Chem., Int. Ed.*, 2015, **54**, 6972–6993.
8 L. Wang, G. Sun, K. Zhang, M. Yao, Y. Jin, P. Zhang, S. Wu and J. Gong, *ACS Sustainable Chem. Eng.*, 2020, **8**, 16781–16790.
9 Y. Park, S. X. M. Boerrigter, J. Yeon, S. H. Lee, S. K. Kang and E. H. Lee, *Cryst. Growth Des.*, 2016, **16**, 2552–2560.
10 P. Sacchi, S. E. Wright, P. Neoptolemou, G. I. Lampronti, A. K. Rajagopalan, W. Kras, C. L. Evans, P. Hodgkinson and A. J. Cruz-Cabeza, *Proc. Natl. Acad. Sci. U. S. A.*, 2024, **121**, e2319127121.
11 D. Hasa, M. Marosa, D.-K. Bučar, M. K. Corpinot, D. Amin, B. Patel and W. Jones, *Cryst. Growth Des.*, 2020, **20**, 1119–1129.
12 S. Huang, V. K. R. Cheemarla, D. Tiana and S. E. Lawrence, *Cryst. Growth Des.*, 2023, **23**, 5446–5461.
13 D. Gogoi, T. Sasaki, T. Nakane, A. Kawamoto, H. Hojo, G. Kurisu and R. Thakuria, *Cryst. Growth Des.*, 2023, **23**, 5821–5826.
14 C. Heffernan, M. Ukrainczyk, J. Zeglinski, B. K. Hodnett and Å. C. Rasmuson, *Cryst. Growth Des.*, 2018, **18**, 4715–4723.
15 C. Darmali, S. Mansouri, N. Yazdanpanah and M. W. Woo, *Ind. Eng. Chem. Res.*, 2019, **58**, 1463–1479.
16 S. J. Urwin, G. Levilain, I. Marziano, J. M. Merritt, I. Houson and J. H. Ter Horst, *Org. Process Res. Dev.*, 2020, **24**, 1443–1456.
17 H. A. Moynihan and D. E. Horgan, *Org. Process Res. Dev.*, 2017, **21**, 689–704.
18 S. Mohamed and L. Li, *CrystEngComm*, 2018, **20**, 6026–6039.
19 S. N. Madanayake, A. Manipura, R. Thakuria and N. M. Adassooriya, *Org. Process Res. Dev.*, 2023, **27**, 409–422.
20 R. Thakuria and A. Nangia, *Cryst. Growth Des.*, 2013, **13**, 3672–3680.
21 N. Tumanova, N. Tumanov, F. Fischer, F. Morelle, V. Ban, K. Robeyns, Y. Filinchuk, J. Wouters, F. Emmerling and T. Leyssens, *CrystEngComm*, 2018, **20**, 7308–7321.
22 G. L. Perlovich, *Cryst. Growth Des.*, 2020, **20**, 5526–5537.
23 S. Aitipamula, P. S. Chow and R. B. H. Tan, *CrystEngComm*, 2014, **16**, 3451–3465.
24 M. R. Ahsan, L. Singh, B. Sar and A. Mukherjee, *Cryst. Growth Des.*, 2024, **24**, 1695–1704.
25 R. Kaur, S. Cherukuvada, P. B. Managutti and T. N. G. Row, *CrystEngComm*, 2016, **18**, 3191–3203.
26 D. Gogoi, K. J. Kalita, N. Biswakarma, M. Arhangelskis, R. C. Deka and R. Thakuria, *RSC Mechanochem.*, 2024, **1**, 452–464.
27 B. Saikia, D. Pathak and B. Sarma, *CrystEngComm*, 2021, **23**, 4583–4606.
28 A. V. Trask, J. van de Streek, W. D. S. Motherwell and W. Jones, *Cryst. Growth Des.*, 2005, **5**, 2233–2241.
29 Z.-H. Li and W.-S. Kim, *Cryst. Growth Des.*, 2024, **24**, 5974–5989.
30 L. S. Germann, M. Arhangelskis, M. Etter, R. E. Dinnebier and T. Friščić, *Chem. Sci.*, 2020, **11**, 10092–10100.
31 L. Casali, L. Mazzei, O. Shemchuk, L. Sharma, K. Honer, F. Grepioni, S. Ciurli, D. Braga and J. Baltrusaitis, *ACS Sustainable Chem. Eng.*, 2019, **7**, 2852–2859.
32 N. M. Adassooriya, S. P. Mahanta and R. Thakuria, *CrystEngComm*, 2022, **24**, 1679–1689.
33 N. H. Madanayake, D. Gogoi, G. K. M. G. Jayasuriya, A. T. D. Perera, R. Thakuria and N. M. Adassooriya, *ACS Sustainable Chem. Eng.*, 2025, **13**, 9481–9489.
34 T. Rajbongshi, S. Parakatawella, D. Gogoi, P. Deka, N. M. Adassooriya and R. Thakuria, *RSC Sustain.*, 2023, **1**, 1416–1422.
35 C. G. Jones, M. W. Martynowycz, J. Hattne, T. J. Fulton, B. M. Stoltz, J. A. Rodriguez, H. M. Nelson and T. Gonen, *ACS Cent. Sci.*, 2018, **4**, 1587–1592.
36 M. A. Spackman and D. Jayatilaka, *CrystEngComm*, 2009, **11**, 19–32.
37 M. A. Spackman and J. J. McKinnon, *CrystEngComm*, 2002, **4**, 378–392.
38 J. J. McKinnon, M. A. Spackman and A. S. Mitchell, *Acta Crystallogr., Sect. B: Struct. Sci.*, 2004, **60**, 627–668.
39 J. J. McKinnon, D. Jayatilaka and M. A. Spackman, *Chem. Commun.*, 2007, 3814–3816.
40 (*a*) A. Bonia, D. Gogoi, N. Kalita, T. Nakane, A. Kawamoto, K. Althubeiti, T. Sasaki, G. Kurisu and R. Thakuria, CCDC 2465561: Experimental Crystal Structure Determination, 2025, DOI: 10.5517/ccdc.csd.cc2nrm79; (*b*) A. Bonia, D. Gogoi, N. Kalita, T. Nakane, A. Kawamoto, K. Althubeiti, T. Sasaki, G. Kurisu and R. Thakuria, CCDC 2465562: Experimental Crystal Structure Determination, 2025, DOI: 10.5517/ccdc.csd.cc2nrm8b; (*c*) A. Bonia, D. Gogoi, N. Kalita, T. Nakane, A. Kawamoto, K. Althubeiti, T. Sasaki, G. Kurisu and R. Thakuria, CCDC 2465472: Experimental Crystal Structure Determination, 2025, DOI: 10.5517/ccdc.csd.cc2nrjcb.